



Different Evolutionary Stages of Massive Star-forming complex S255IR

Yuan Wang^{1,2}, Henrik Beuther², Arjan Bik², Zhibo Jiang¹, and Thomas Henning²



ywang@pmo.ac.cn

¹Purple Mountain Observatory, CAS
²Max-Planck-institute for Astronomy

Abstract

We present spectral line and continuum data at mm and NIR wavelength for three regions of high-mass star formation in different evolutionary stages: While we find multiple mm continuum sources toward all regions, their outflow, disk and chemical properties vary considerably between them. For example, the most evolved source S255IR exhibits a beautiful collimated bipolar outflow visible in CO (SMA results) and H₂ emission (SINFONI results), the outflows from the youngest region S255S are still small and rather confined in the region of the mm continuum peaks. Also the chemistry toward S255IR is most evolved exhibiting strong emission from complex molecule, while much fewer molecular lines are detected in S255N, and in S255S we detected only CO isotopologues and SO lines. Furthermore, a comparison of the NIR SINFONI and mm data from S255IR clearly reveal two different (proto) stellar populations with an estimated age difference of approximately 1 Myr.

Introduction: The massive star-forming complex S255IR is embraced by the Sharpless regions S255 and S257, which are already evolved HII regions (Fig. 1). The SCUBA 850 micron observation shows three main continuum sources: S255IR in the center (a.k.a. IRAS06099+1800), and two additional mm continuum peaks toward the north and south (Klein et al. 2005), which will be labeled as S255N and S255S (Fig. 1). In a concerted effort from near infrared to mm wavelengths, we studied the three massive star formation regions S255IR/N/S, with the Submillimeter Array (SMA), IRAM 30m and the VLT-SINFONI.

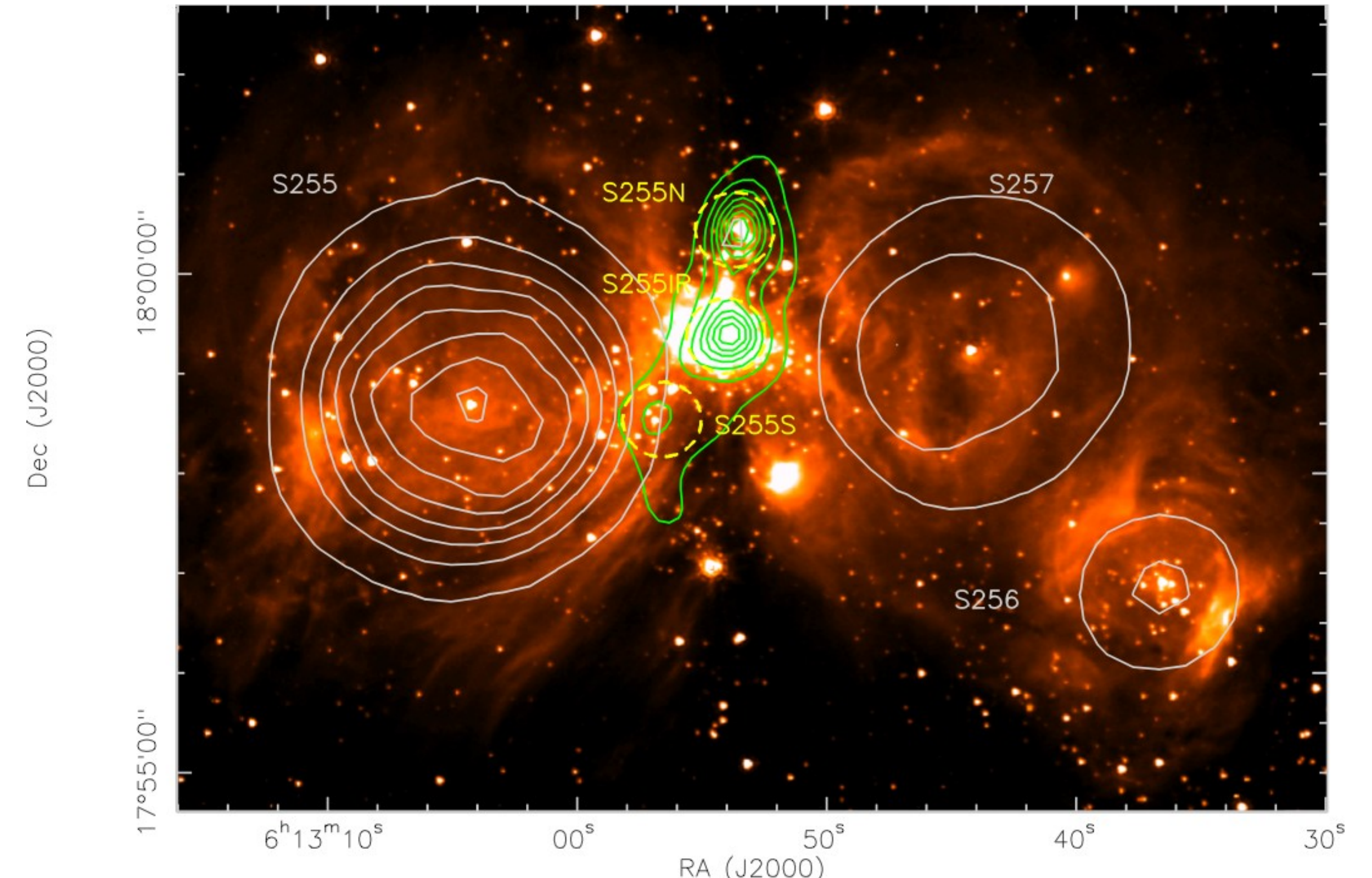


Figure 1. SPITZER 8 micron image overlaid with SCUBA 850 micron contours (green) and NVSS 1.4 GHz contours (white). The yellow circles mark the three regions we observed with the SMA.

Dust continuum, Outflow properties and rotational structures

Figure 2 shows the dust continuum and the outflow maps of the three sub-regions. The two stars in the top left panel mark the NIR sources: NIRS 3 and NIRS 1, and NIRS 1 has been identified as a massive disk candidate by NIR polarization observation (Jiang et al. 2008). We found all the three regions fragmented into several sub sources and all contain molecular outflows, however they also show distinctively different properties. S255IR, the most developed region, shows a collimated outflow associated with S255IRmm1, which is also associated with Class II CH₃OH masers and H₂O masers. In the younger regions S255N and S255S, the outflows are rather confined in the region of the mm continuum peaks.

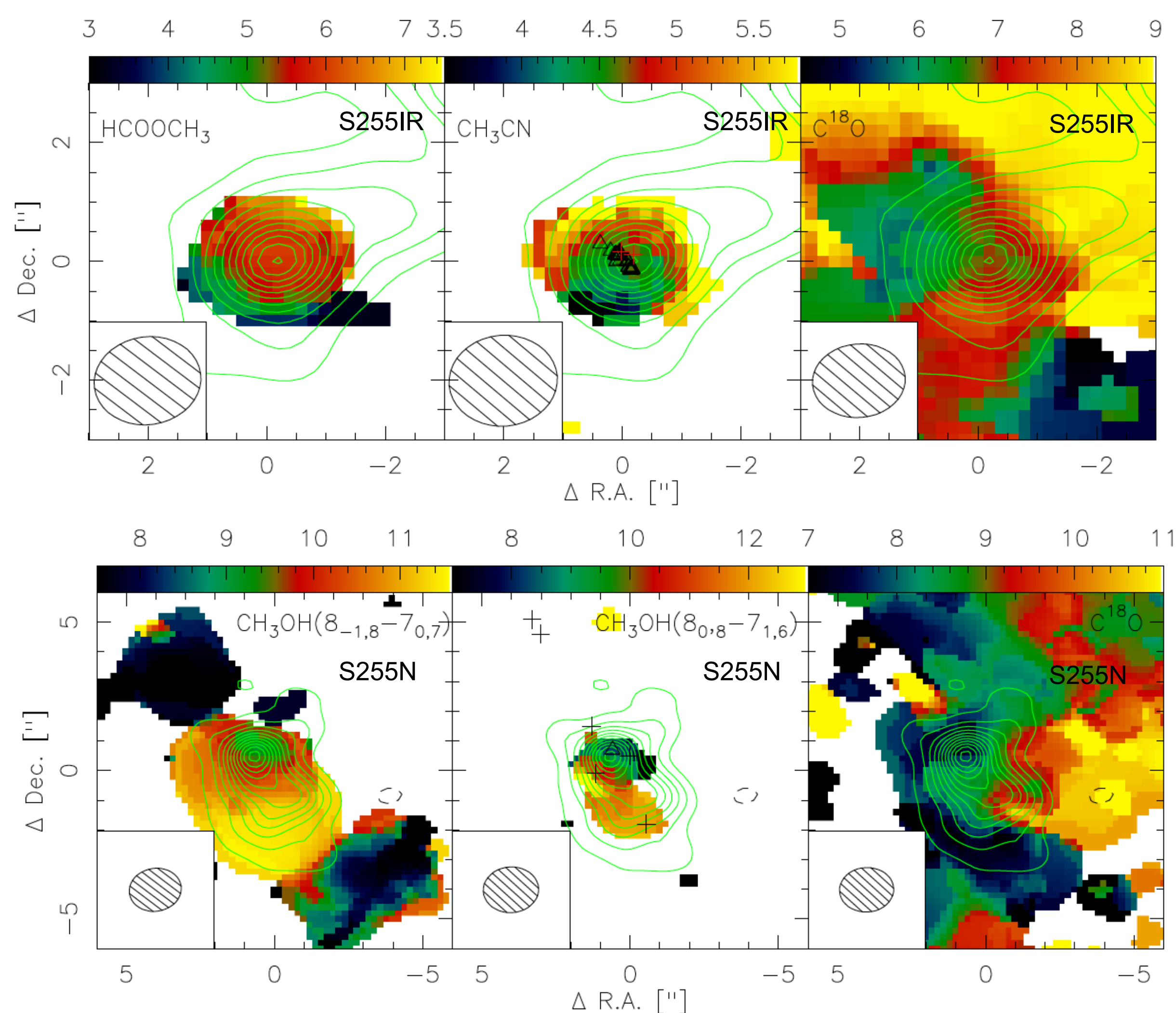


Figure 3. The first moment map of S255IR (top panel) and S255N (bottom panel). The triangles in the S255IR panel (top) are water masers (Goddi et al. 2007) and the red crosses are 6.7 GHz CH₃CN masers (Xu et al. 2009). The crosses in the S255N panel (bottom) mark the position of the Class I methanol masers (Kurtz et al. 2004) and the triangle is the water maser (Cyganowski et al. 2007).

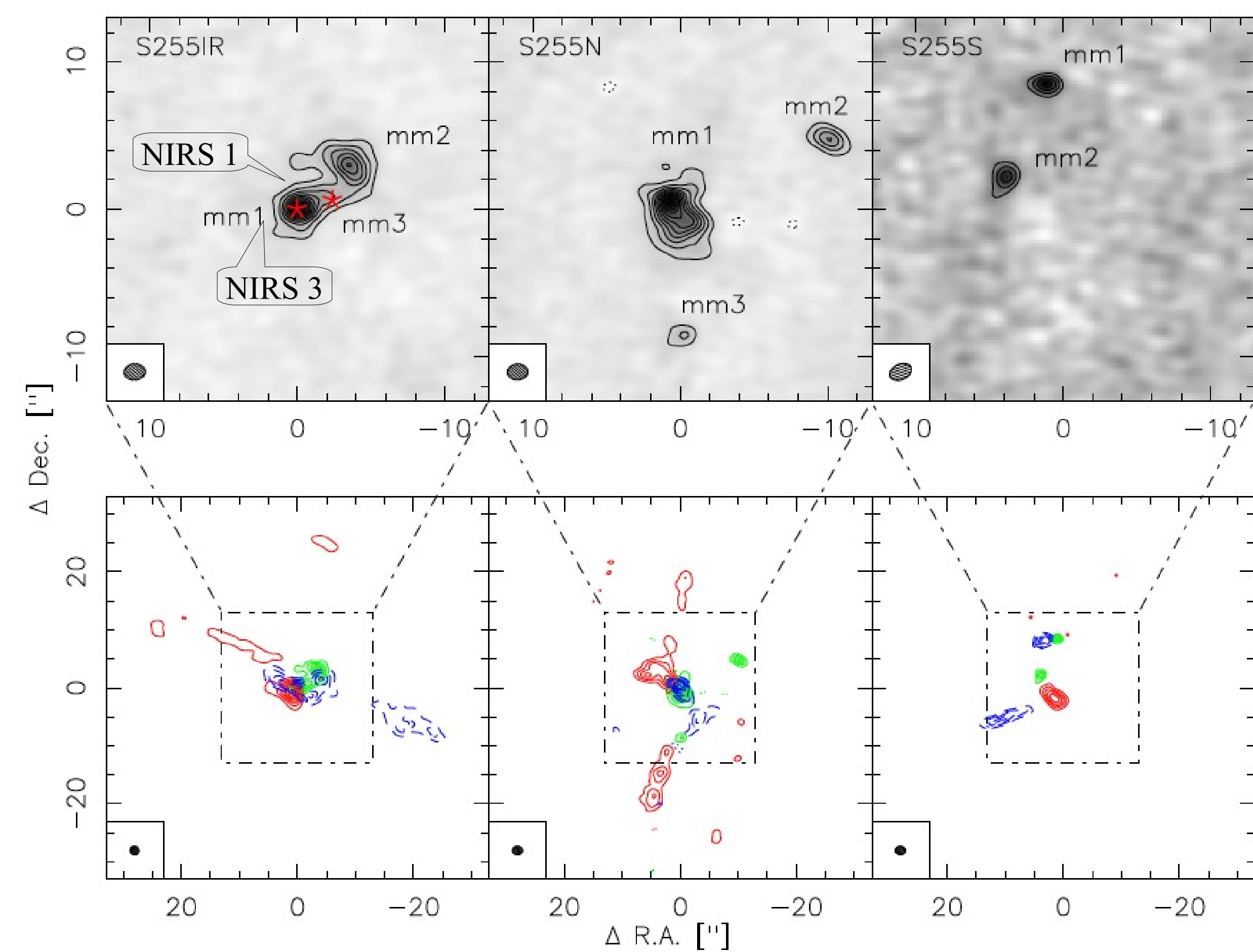


Figure 2a. Dust continuum map of the three regions.

Figure 2b: Dust continuum maps overlaid with outflows contours.

Red: red-shifted
Blue: blue-shifted
Green: continuum

Figure 3 presents the first moment maps of S255IR (top) and S255N (bottom). In the top panel, the HCOOCH₃ and CH₃CN first moment maps both indicate a velocity gradient perpendicular to the direction of the outflow (see the left panel in Fig. 2b), which indicates the existence of a rotational structure. The proper motions of the water masers also indicate the same rotational structure (Goddi et al. 2007). Due to the missing of short spacing information or high optical depth of C¹⁸O, we cannot find this velocity gradient in the C¹⁸O first moment map. In the S255N panel (bottom), the two CH₃OH first moment maps also show a velocity gradient perpendicular to the direction of the outflow (see the middle panel in Fig. 2b), which indicates a rotational structure. Also the Class I CH₃OH masers follow the direction of the outflow from this source. Due to the same reason as in S255IR, we also find the similar velocity gradient in S255N.

Different populations in S255IR

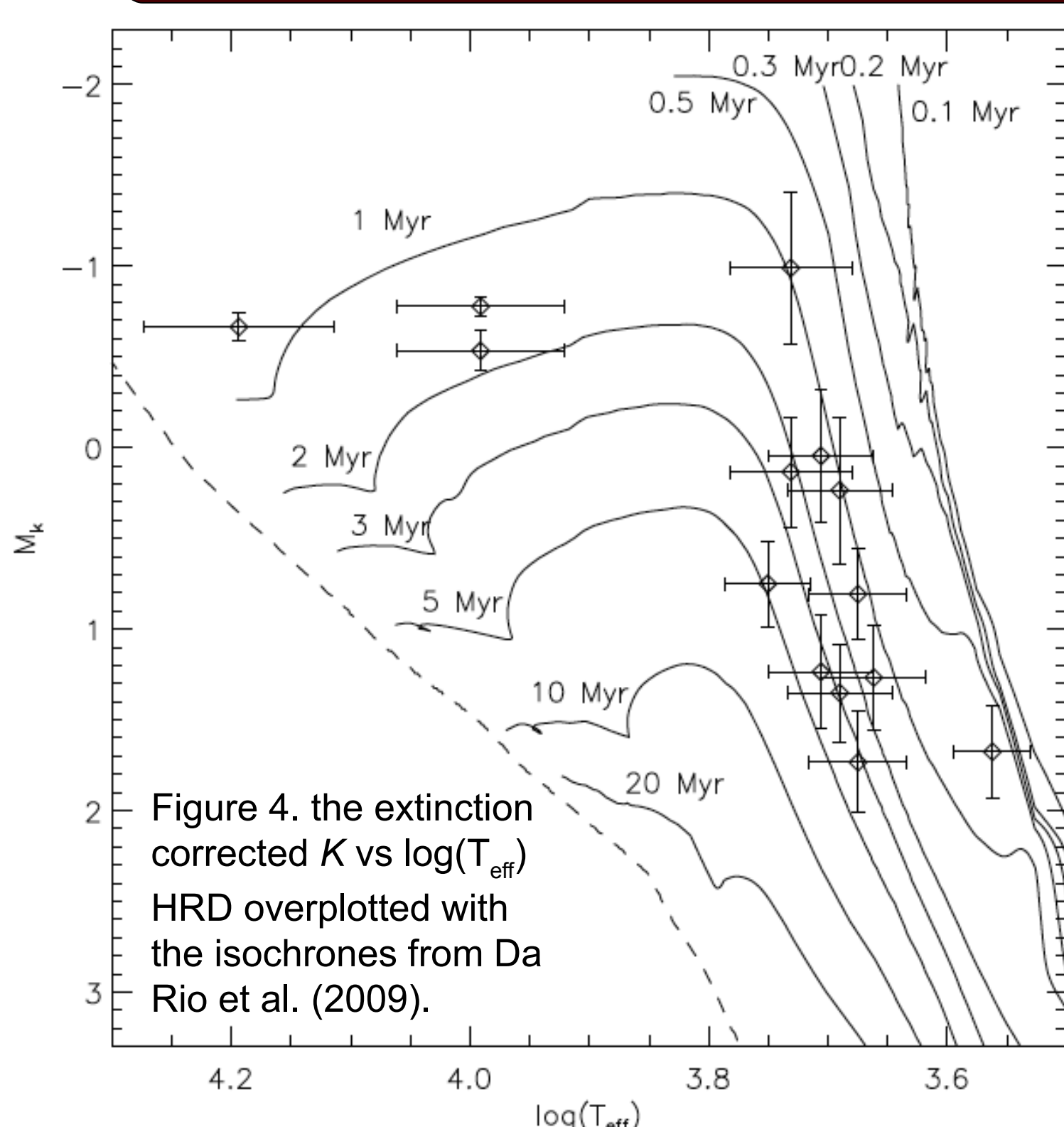


Figure 4. the extinction corrected K vs $\log(T_{\text{eff}})$ HRD overlaid with the isochrones from Da Rio et al. (2009).

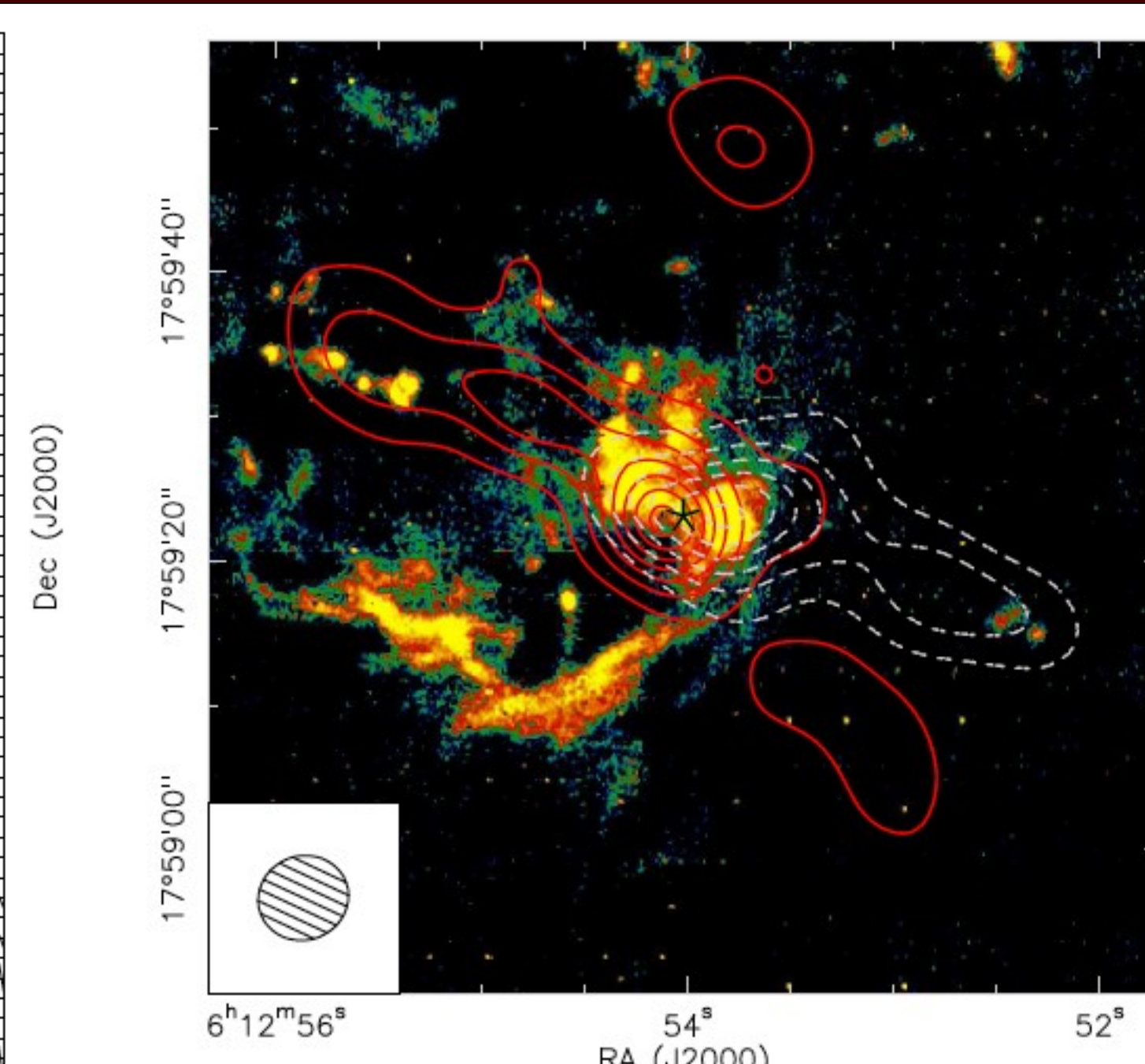


Figure 5. The SINFONI H₂ line emission overlaid with SMA combined with 30 m CO outflow. Red is red shifted and dashed is blue shifted. The star marks the position of the continuum peak.

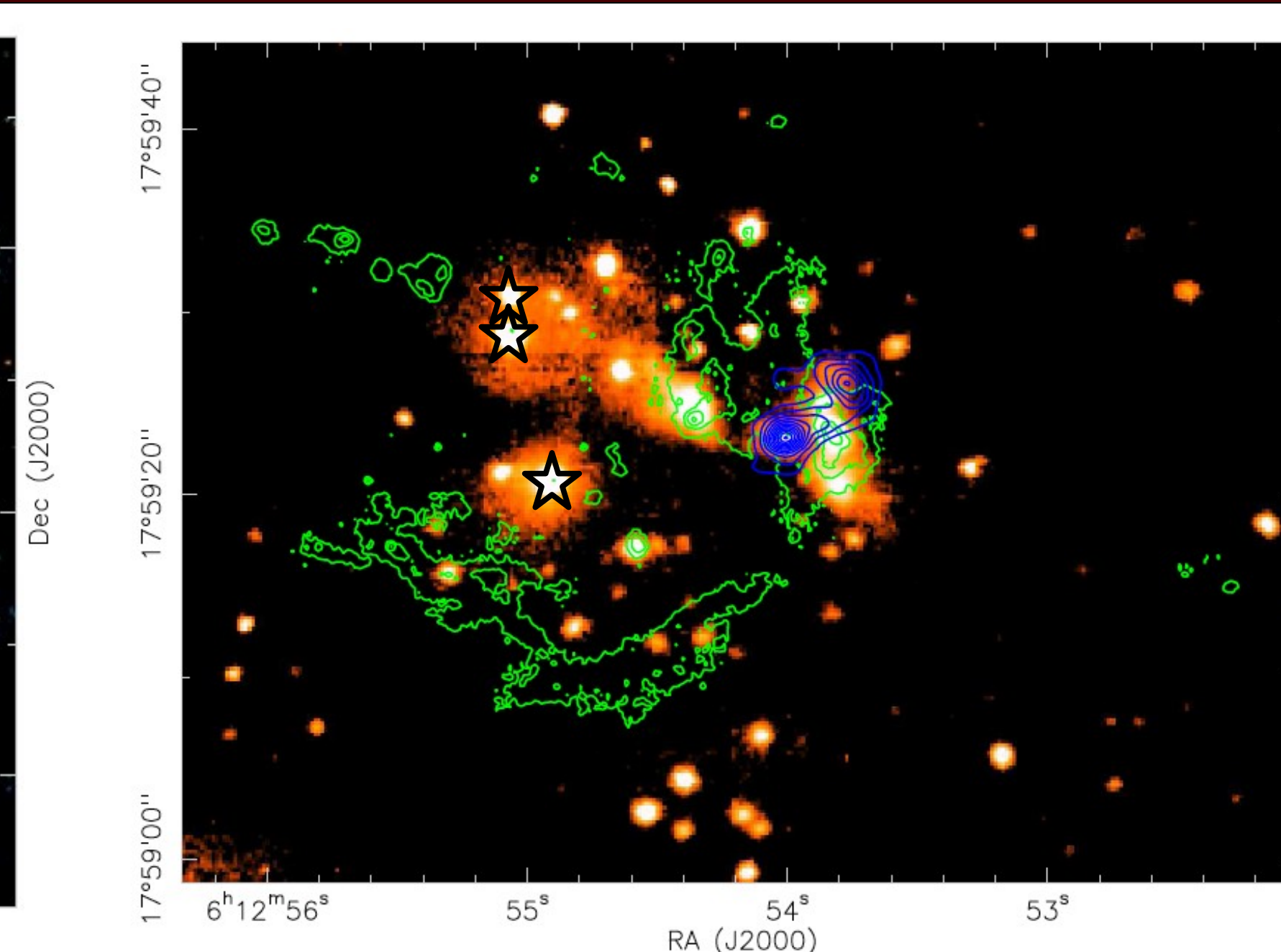


Figure 6. The SINFONI Bry continuum map overlaid with H₂ line emission (green contours, the same emission as Fig. 5) and the SMA continuum (blue contours). The three stars mark the late B early A stars in the cluster.

From the SINFONI $H+K$ spectra, we got the spectral type of the IR cluster members (Fig. 4 and Fig. 6), except NIRS 3 and NIRS 1, which have strong envelope dust emission and can not be classified. The HRD (Fig. 4) show the age of the IR cluster is around 1 to 4 Myr, which is much older compared to our mm sources with an estimated age $\leq 10^5$ yr based on outflow data. And the three late B early A stars (marked with three stars in Fig. 6) that are the most massive ones in the cluster (besides our mm sources) are at the top left corner of the HRD and younger than other low mass sources. And combined with our mm sources, we found that, while the most massive sources in the cluster are still deeply embedded with on going formation process, there is

already a formed low mass cluster, which indicates that the low mass stars are formed firstly and the massive ones are formed much later. The whole cluster revealed two populations of stars.

- References:
- Cyganowski, C. J., Brogan, C. L., & Hunter, T. R. 2007, AJ, 134, 346
 - Goddi, C., Moscadelli, L., Sanna, A., Cesaroni, R., & Minier, V. 2007, A&A, 461, 1027
 - Jiang, Z., Tamura, Hoare, M. G., et al. 2008, ApJ 673, L175
 - Klein, R., Posselt, B., Schreyer, K., Forbrich, J., & Henning, T. 2005, ApJS, 161, 361
 - Kurtz, S., Hofner, P., & Alvarez, C. V. 2004, ApJS, 155, 149
 - Xu, Y., Voronkov, M. A., Pandian, J. D., et al. 2009, A&A, 507, 1117
 - Da Rio, N., Gouliermis, D. A., & Henning, T. 2009, ApJ, 696, 528